

Respiration-averaged CT versus standard CT attenuation maps for correction of ^{18}F -NaF uptake on hybrid PET/CT

Evangelos Tzolos^{a, b*}, Martin Lyngby Lassen^{a*}, Tinsu Pan^c, Jacek Kwiecinski^{a, d},
Sebastien Cadet^a, Damini Dey^a, Marc R Dweck^b, David E Newby^b, Daniel Berman^a,
Piotr Slomka^a

a Department of Imaging (Division of Nuclear Medicine), Medicine, and Biomedical Sciences, Cedars-Sinai Medical Center, Los Angeles, CA, USA;

b BHF Centre for Cardiovascular Science, University of Edinburgh, Edinburgh, United Kingdom

c Department of Imaging Physics, The University of Texas M.D. Anderson Cancer Center, Houston, Texas

d Department of Interventional Cardiology and Angiology, Institute of Cardiology, Warsaw, Poland

*equal contribution as first author

Address for Correspondence:

Piotr J. Slomka, PhD

Artificial Intelligence in Medicine Program

Cedars-Sinai Medical Center

8700 Beverly Blvd, Ste A047N

Los Angeles, CA 90048, USA

Email: piotr.slomka@cshs.org Phone: 310-423-4348 Fax: 310-423-0173

Funding

This research was supported in part by grant R01HL135557 from the National Heart, Lung, and Blood Institute/National Institutes of Health (NHLBI/NIH). The study was also supported by a grant (“Cardiac Imaging Research Initiative”) from the Miriam & Sheldon G. Adelson Medical Research Foundation. None of the other authors have any conflict of interest relevant to this study.

Abstract

Purpose

To evaluate the impact of a respiratory averaged computed tomography attenuation correction (RACTAC) instead of a standard single-phase computed tomography (CT) attenuation correction (CTAC) map on the quantitative measures of coronary ^{18}F -NaF uptake in PET/CT.

Methods

This study comprised 23 patients who underwent ^{18}F -NaF coronary PET in a hybrid PET/CT system, employing ^{18}F -NaF (250MBq). All patients had two CT scans, a standard single-phase CTAC obtained during free-breathing, and a 4D cine-CT scan. From the Cine-CT acquisition, RACTAC maps were obtained by averaging all images acquired over 5 seconds. Two PET reconstruction protocols, one employing CTAC and another employing RACTAC for attenuation correction were considered in this study. Following reconstruction, the quantitative impact of employing RACTAC was assessed using maximum target-to-background (TBR_{MAX}) and coronary microcalcification activity (CMA). Statistical differences were analyzed using reproducibility coefficients and Bland-Altman plots.

Results

In 23 patients, we evaluated 34 coronary lesions using PET reconstructions utilizing CTAC and RACTAC. There was good agreement between CTAC and RACTAC PET reconstructions for TBR_{MAX} (median [Interquartile range, IQR]: CTAC = 1.65[1.23-2.38], RACTAC = 1.63[1.23-2.33], $p=0.55$), with coefficient of reproducibility of 0.18. The CMA

agreement was similar (median [IQR]: CTAC = 0.10 [0-1.0], RACTAC= 0.15[0-1.03],
p=0.55 with coefficient of reproducibility of 0.17

Conclusion

Employing RACTAC maps does not affect the quantification of the coronary ^{18}F -NaF uptake on PET/CT.

Keywords: Respiration-averaged CT attenuation correction, Motion correction, PET/CT, Cardiac PET, ^{18}F -sodium fluoride, Vulnerable plaque, Coronary Microcalcification Activity

Abbreviations

RACTAC respiration-averaged CT attenuation correction

CTAC CT attenuation correction

CMA coronary microcalcification activity

¹⁸F-NaF ¹⁸F-sodium fluoride

PET positron emission tomography

CTA computed tomography angiography

ECG-MC cardiac motion corrected

BC background blood pool clearance correction

TBR_{MAX} maximum target to background ratio

SUV_{MAX} maximum standardized uptake value

VOI volume of interest

Introduction

Hybrid positron emission tomography and computed tomography (PET/CT) imaging with ^{18}F -sodium fluoride (^{18}F -NaF) has been successfully employed for the assessment of atherosclerotic disease activity in the coronary arteries and can potentially identify high-risk plaques (1-4).

Currently, hybrid ^{18}F -NaF PET/CT scans are obtained utilizing a 30 min PET acquisition in listmode format, followed by PET image reconstructions employing four or ten cardiac phases with either breath-hold or free-breathing CT attenuation correction (CTAC) maps (5-7). Previous studies on myocardial perfusion and viability have shown that misalignment of the PET emission data and the CTAC maps pose risks of false-positive findings in the clinical setting (8, 9), with loss in the predictive value if not corrected for motion (10). To ameliorate this issue, realignment of the CTAC maps and PET emission data can be performed when necessary, before PET image reconstruction to get optimal predictive value(11). However, single-phase CTAC maps have been shown to affect the quantitative accuracy of myocardial viability studies owing to the continuous respiratory translations during the PET emission acquisitions(12-15). Previous studies employing respiratory averaged CTAC maps (RACTAC), obtained from cine-CT scans have shown to improve the quantitative accuracy in myocardial perfusion and viability studies(16, 17). Recently, ^{18}F -NaF PET has been established as a non-invasive imaging modality to identify high-risk and ruptured coronary atherosclerotic plaques(1, 3, 18, 19). Quantitative accuracy and reproducibility of imaging this tracer will be critical to establish its clinical value. However, the quantitative accuracy of lesion

micro-calcification activity assessed with ^{18}F -NaF PET and RACTAC for attenuation correction has not yet been evaluated.

In this study, we aimed to evaluate the quantitative impact of utilizing RACTAC on ^{18}F -NaF uptake measurements and compare RACTAC to PET images reconstructed using routinely acquired CTAC maps. To this end, we aimed to compare the quantification of individual lesions utilizing target-to-background ratios (TBR) and whole-vessel (and entire coronary tree) microcalcification burden using coronary microcalcification activity (CMA) assessments(2).

Materials and Methods

Study population

Twenty-three patients underwent hybrid ^{18}F -NaF PET/CT examinations of the coronary arteries as part of the ongoing Effect of Evolocumab on Coronary Artery Plaque Volume and Composition by CCTA and Microcalcification by ^{18}F -NaF PET study (NCT03689946)(20). Inclusion in the study required a Coronary Computed Tomography Angiography (CCTA) confirmed high noncalcified coronary artery plaque volume ($>440\text{ mm}^3$). Exclusion criteria were as follows: renal dysfunction (creatinine $> 1.5\text{ mg/dL}$) prior to imaging, history of allergy to iodine contrast agents, allergy to evolocumab, women who are breastfeeding, active atrial fibrillation, history of coronary artery bypass graft, inability to lie flat, inability or unwilling to give informed consent, major illness or life expectancy <1 year, planned coronary revascularization or major non-cardiac surgery in the next 12 months, previous or current evolocumab use.

Imaging protocol

CCTA acquisition

The CCTA was acquired the same day as the PET scan for 13 patients, while the remaining cases (n=10) had the CCTA within 21 days (range=2-21 days). All patients were scanned with arms positioned above the head in a 192-slice Somatom Force Dual Source mCT system (Siemens Healthineers, Knoxville, TN, USA). The CCTA imaging parameters included prospective gating, 250 ms rotation time, body-mass index (BMI) dependent voltage (<25 kg/m², 100 kV; ≥25 kg/m², 120 kV), and tube-current time product of 160–245 mAs. Patients were administered beta-blockers (orally or intravenously) to achieve a target heart rate of <60 beats/min, followed by a BMI-dependent bolus-injection of contrast media (400 mg/mL) with a flow of 5–6 mL/s after determining the appropriate trigger delay defined by a test bolus of 20 mL of contrast material.

PET acquisition

Following the CCTA acquisition (at the same day or different day within a 21 days period as described above), all patients underwent ¹⁸F-NaF positron emission tomography (PET), with arms positioned above the head, on a hybrid PET-CT scanner (Discovery 710, GE Healthcare, Milwaukee, WI, USA). Prior to imaging, subjects were administered with a target dose of 250 MBq of ¹⁸F-NaF and rested in a quiet environment for 180 min (**Figure 2**).

First, we acquired an anteroposterior scout at 100kV and 10mA with a field of view of 21 mm starting from the pulmonary artery bifurcation and extending to the diaphragm. Then 4D cine-CT data were acquired with the following settings: 120 kV, 10 mA, field of view 50 cm, slice thickness 2.5 mm and cine duration of 5 s with the respiratory trace during

the scan recorded by the respiratory management tool (RPM) from Varian. After cine-CT, a standard AC map was acquired at the following settings: 100kV, 40mAs/rotation, 0.5s rotation, 1.375 mm/rotation pitch and 5mm slice thickness. Finally, PET acquisition was performed in list mode for 30 minutes.

RACTAC map From the CINE CT acquisition, we created RACTAC maps from averaging the CT images in 5 seconds. (**Figure 1**). Both the CTAC and the RACTAC maps were used for attenuation correction using a vendor-provided reconstruction toolbox.

PET reconstruction The acquired electrocardiography-gated raw data (list mode dataset) was reconstructed using a standard ordered expectation-maximization algorithm with time of flight, and resolution recovery using 4 cardiac bins. All images were reconstructed using a 256×256 matrix (47 slices) employing 4 iterations with 5-mm post filtering and 24 subsets.

Two series of PET images, one employing CTAC and another with RACTAC, were reconstructed into 4 cardiac phases using a vendor-provided software (REGRECON-REL5, General Electric, Wisconsin, USA).

Post reconstruction Cardiac motion correction Cardiac motion-corrected images were obtained from the gated PET reconstructions through PET-PET image co-registration using a diffeomorphic registration(21). This technique enables alignment of all gates to the end-diastolic position and as a result, allows for inclusion of all PET counts

acquired. We used dedicated coronary PET imaging software for image analysis (FusionQuant, Cedars-Sinai Medical center)(18).

PET quantification

Background blood pool clearance correction

To minimize the impact of variations in background blood pool activity introduced by variations in the injection-to-scan delays (6, 7), we standardized the background blood pool activity to an injection-to-scan delay of 180 minutes using a previously described correction factor (6) (Eq. 1)

$$\text{SUV}_{\text{Background corrected}} = \text{SUV}_{\text{Background}} * e^{(-0.004 * (180 - t))} \quad (1)$$

where t represents the injection-to-scan delay in minutes.

TBR_{MAX} quantification

TBR_{MAX} was obtained using a previously described protocol (2). In brief, the ¹⁸F-NaF uptake in atherosclerotic lesions was evaluated in a 3D spherical volume of interest (VOI) (radius 5 mm). In all plaques, the maximum standardized uptake values (SUV_{MAX}) were measured within manually drawn regions of interest. TBR_{MAX} values were calculated by dividing the coronary SUV_{MAX} by the blood pool activity measured in the right atrium (cylindrical volume of interest radius 10 mm and thickness 5 mm) at the level of the right coronary artery ostium. Lesion SUV_{max} and TBR_{max} were evaluated using the same VOIs for both reconstructions, using delineations inserted on PET images reconstructed using CTAC.

CMA quantification

To obtain the CMA(2) values, two distinct steps were performed. First, we selected the proximal and distal end of the vessel (>2 mm) and applied a vessel tracking algorithm to extract whole-vessel tubular 3D volumes of interest from CCTA using dedicated semi-automated Autoplaque software (Cedars-Sinai Medical Center, Los Angeles, CA)(22). In a tubular VOI, along the extracted centerlines, with 4-mm diameter, we measured the coronary microcalcification activity (CMA) on the PET/CT co-registered images. CMA was defined as the average SUV within the activity volume above a threshold established as the mean background SUV +2 standard deviations. The background activity was measured in the right atrium. In order to evaluate the total uptake, we added the CMA activity of all epicardial vessels (CMA_{total}).

Offset calculation between CTAC and RACTAC

Translations of the CTAC and RACTAC maps were calculated for all patients as the 3D offset, using the aortic valve as a point of reference.

Statistical analysis

The data were tested for normality using the Shapiro–Wilk test. Statistical analysis was performed using MedCalc Statistical Software version 19.1.7 (MedCalc Software bv, Ostend, Belgium). Continuous, normally distributed variables were presented as mean \pm SD (standard deviation), whereas non-normally distributed continuous data were presented as median [range]. We assessed CMA and TBR_{MAX}, using descriptive statistics and Bland–Altman plots, as well as coefficients of reproducibility. Boxplots were designed using R 3.5.0 and statistical significance of the difference between the correlated

variances was calculated using the Pitman Morgan test; a two-sided p value <0.05 was considered significant.

Results

Twenty-three patients underwent hybrid ^{18}F -NaF PET/CT examinations of the coronary arteries. A total of 34 coronary lesions were identified on reconstructions on both PET corrected with CTAC and RTAC maps (**Figure 3**). Patient demographics are shown in **Table 1**. Across all patients, the median (IQR) offset for the CTAC and RACTAC maps were calculated to be 5.4mm (2.2 mm – 9.9mm).

Per-lesion analyses (TBR)

TBR values obtained using the same delineation of the lesions for reconstructions employing CTAC and RACTAC were similar (median TBRmax [Interquartile range; IQR]: CTAC = 1.65 [1.23-2.38], RACTAC = 1.63 [1.23-2.33], $p = 0.55$). (**Figure 4, A**). Good agreement of the TBR measures obtained using the two different attenuation correction techniques was observed with coefficient of reproducibility of 0.18 (**Figure 4, B**).

Per vessel analyses (CMA)

Assessments of the individual vessel microcalcification burden (CMA) revealed non-significant differences between PET images reconstructed using CTAC and RACTAC scans (median [IQR] CMA: CTAC = 0.10 [0-1.0], RACTAC = 0.15 [0-1.03], $p = 0.19$) (**Figure 5, A**). Bland-Altman plots of the CMA values revealed a high degree of agreement when comparing the per vessel burden (**Figure 5, B**), with coefficient of reproducibility of 0.17.

Coronary tree analyses (CMA)

Whole-coronary tree microcalcification burden (CMA for all three vessels combined), was found to be comparable for the two series of reconstructions (CMA_{total}: median [IQR]: CTAC = 1.01 [0-1.83], RACTAC = 1.05 [0-1.95], $p=0.42$) (**Figure 6, A**). In concordance with the single-vessel CMA burden, the data reconstructed using the two attenuation correction protocols were in agreement (**Figure 6, B**), with a coefficient of reproducibility of 0.17.

Discussion

In this study, we evaluated the impact of using standard CTAC maps and RACTAC maps obtained from cine-CT maps through respiratory averaging of CT data obtained in 4D on coronary PET. Our main finding was that using RACTAC did not introduce any significant changes in the quantitative comparisons, both when comparing single lesion activities and vessel and the whole coronary tree microcalcification burden. To our knowledge, this is the first study evaluating RACTAC maps in the assessment of coronary PET/CT.

Quantitative accuracy is of high importance in the assessment of both the singular vulnerable plaque and in the overall assessment of the coronary tree microcalcification burden (2). Previous studies have shown that both inter-reader and inter-scan variabilities are within acceptable ranges(6, 23). However, the quantitative accuracy has been shown to be impaired by significant respiratory and patient motion shifts during the acquisition

(6, 24). Despite significant improvements in the test-retest reproducibility and reclassification of singular lesions following the introduction of sophisticated motion correction techniques, the quantitative accuracy might still be impaired by respiratory translations of the PET images during the 30 min long PET acquisitions. Current attenuation correction protocols employ a single-phase CT scan (free breathing, or end-expiratory breathing) (5, 12-15). The use of single-phase CTAC maps may change the observed uptake patterns in the heart, with deviations between 6% in canine models (25), and as much as 35% in human studies (26).

To minimize potential mismatches, other groups have explored the possibility of scanning at an optimal time during respiration (27-29). Unfortunately, even with perfect breath instructions, it is challenging to state the optimal breath protocol applicable for all patients and even if the CT scan was obtained at the optimal breathing state. Pan et al.(17, 30) demonstrated that potential misalignment caused by different breathing phases during helical CT and PET affects both the quantitative and qualitative accuracy. By utilizing RACTAC for attenuation correction instead of the commonly employed CTAC, the frequency and impact of breathing artefacts were reduced, with improved tumor quantification as a result (16). It was argued that by utilizing, fast-scan cine CT acquisition of 5 seconds it is possible to bring together the temporal resolutions of CT and PET (16, 17, 30).

In this study, however, we did not observe any significant changes in PET uptake values between the reconstructions obtained using CTAC and RACTAC. This finding is different from previous reports (8, 17, 25) where up to 40% of the false-positive results normalized with the use of respiratory averaged CTAC maps (8). This could be explained by several

reasons. Firstly, the investigators were measuring the activity of the myocardium and because of the higher diaphragmatic position at end-expiration they observed more misregistration artefacts resulting in decreased emission activity in inferior, inferoseptal, and inferolateral walls and compromised quantitative accuracy and the interpretation of myocardial viability. These artefacts were corrected by using respiratory-gated average attenuation maps. In our study, we concentrated on focal activity away from the diaphragm and did not observe a difference in coronary ^{18}F -NaF uptake between the single-phase CTAC and respiratory averaged CTAC.

Secondly, in these studies, the investigators measured the average activity, while we measured maximum activity (TBR_{MAX}) or activity above a specific threshold (CMA). By measuring maximum activity, we have encountered less variability by potential motion-driven misregistration as our volume of interest had a diameter of 5 mm. Gould et al.(8) showed that it was the transaxial misregistration of >6 mm that frequently caused artefactual defects and therefore by applying a volume of interest of 5 mm and measuring maximal activity we encountered less variability in our measurements.

Thirdly, the median offset of the CTAC and RACTAC images were of magnitude of 5.4mm (3D), with only 5 patients having translations of more than 10mm between the CTAC and RACTAC maps. These minor offsets, combined with the averaging of the attenuation correction maps result in a relatively small impact of RACTAC images when compared to the CTAC maps.

Finally, we used cardiac motion-corrected reconstructions(5) improving our ability to discriminate activity coming from the corresponding plaque lesion and improving our co-registration. We have previously shown that cardiac motion causes attenuation artifact

and therefore correcting for cardiac motion improves our ability to detect coronary artery disease on myocardial perfusion scans(31). Such cardiac motion correction was not used in previous RACTAC work with myocardial perfusion scans(32). In particular, the effects of cardiac contraction exceed that of respiration with regards to the displacement of the coronaries (cardiac contraction displaces the coronary arteries 8–26mm during the cardiac cycle, while normal respiration leads to movement of the heart of approximately 6–13mm (33).

The coefficient of reproducibility reported in this study is similar to findings reported in test-retest reproducibility studies where both similar interscan variations (6), and inter-reader variations we observed(23). While these results have focused on the test-retest and inter-reader variability for two different studies, our current study reports variations occurring as a result of the attenuation correction. The main finding of this study is that the variations added to the quantitative assessments of the per-lesion and whole coronary tree microcalcification burden are within the range of the reported variations. Therefore, RACTAC applied to the coronary plaque assessments does not seem to change the quantitative ^{18}F -NaF PET results when compared to the standard CTAC technique.

Limitations

Our study has limitations. Firstly, our sample is small (23 patients). Despite that, we showed that our reproducibility coefficient is below the previously reported interobserver and interscan variation (23). Secondly, we report results obtained using cardiac motion correction which have less noise and lower TBR values than the commonly presented end-diastolic imaging reconstruction(1, 19). However, previous studies from our group have shown that both end-diatstolic and cardiac motion corrected images can be used

for ^{18}F -NaF coronary uptake assessments(5, 6). Finally, this is a single-center study and we used only scanners from one vendor, thus, vendor-specific variations cannot be ruled out. A bigger study involving multiple centers and readers would be required to confirm our findings.

New Knowledge Gained

Using RACTAC instead of CTAC maps does affect quantitative accuracy of ^{18}F -NaF PET/CT uptake. This finding is important to ensure the optimal quantitative accuracy in studies utilizing ^{18}F -NaF, such as PREFFIR [NCT02278211], where standard CTAC maps are employed. Based on this finding, given a comparable quantitative accuracy of CTAC and RACTAC maps, both approaches can be used depending on the institutional acquisition protocols.

Conclusion

Applying respiration-averaged CT attenuation correction (RACTAC) maps do not affect the quantification of the coronary lesions as read in fusion PET/CT images. Current protocols utilizing single-shot CTAC maps provide equivalent corrections for the clinical reading of the patients.

References

- (1) Joshi NV, Vesey AT, Williams MC, Shah AS, Calvert PA, Craighead FH et al. 18F-fluoride positron emission tomography for identification of ruptured and high-risk coronary atherosclerotic plaques: a prospective clinical trial. *Lancet* 2014;383:705-13.
- (2) Kwiecinski J, Cadet S, Daghem M, Lassen ML, Dey D, Dweck MR et al. Whole-vessel coronary (18)F-sodium fluoride PET for assessment of the global coronary microcalcification burden. *Eur J Nucl Med Mol Imaging* 2020.
- (3) Kwiecinski J, Dey D, Cadet S, Lee SE, Tamarappoo B, Otaki Y et al. Predictors of 18F-sodium fluoride uptake in patients with stable coronary artery disease and adverse plaque features on computed tomography angiography. *Eur Heart J Cardiovasc Imaging* 2019.
- (4) Kwiecinski J, Slomka PJ, Dweck MR, Newby DE, Berman DS. Vulnerable plaque imaging using 18F-sodium fluoride positron emission tomography. *The British Journal of Radiology* 2019;20190797.
- (5) Doris MK, Otaki Y, Krishnan SK, Kwiecinski J, Rubeaux M, Alessio A et al. Optimization of reconstruction and quantification of motion-corrected coronary PET-CT. *J Nucl Cardiol* 2018.
- (6) Lassen ML, Kwiecinski J, Dey D, Cadet S, Germano G, Berman DS et al. Triple-gated motion and blood pool clearance corrections improve reproducibility of coronary (18)F-NaF PET. *Eur J Nucl Med Mol Imaging* 2019;46:2610-20.
- (7) Kwiecinski J, Berman DS, Lee SE, Dey D, Cadet S, Lassen ML et al. Three-Hour Delayed Imaging Improves Assessment of Coronary (18)F-Sodium Fluoride PET. *J Nucl Med* 2019;60:530-5.
- (8) Gould KL, Pan T, Loghin C, Johnson NP, Guha A, Sdringola S. Frequent diagnostic errors in cardiac PET/CT due to misregistration of CT attenuation and emission PET images: a definitive analysis of causes, consequences, and corrections. *J Nucl Med* 2007;48:1112-21.
- (9) Martinez-Moller A, Souvatzoglou M, Navab N, Schwaiger M, Nekolla SG. Artifacts from misaligned CT in cardiac perfusion PET/CT studies: frequency, effects, and potential solutions. *J Nucl Med* 2007;48:188-93.
- (10) Slomka PJ, Rubeaux M, Le Meunier L, Dey D, Lazewatsky JL, Pan T et al. Dual-Gated Motion-Frozen Cardiac PET with Flurpiridaz F 18. *J Nucl Med* 2015;56:1876-81.
- (11) Slomka PJ, Diaz-Zamudio M, Dey D, Motwani M, Brodov Y, Choi D et al. Automatic registration of misaligned CT attenuation correction maps in Rb-82 PET/CT improves detection of angiographically significant coronary artery disease. *Journal of nuclear cardiology : official publication of the American Society of Nuclear Cardiology* 2015;22:1285-95.
- (12) Loghin C, Sdringola S, Gould KL. Common artifacts in PET myocardial perfusion images due to attenuation-emission misregistration: clinical significance, causes, and solutions. *J Nucl Med* 2004;45:1029-39.
- (13) Koshino K, Fukushima K, Fukumoto M, Sasaki K, Moriguchi T, Hori Y et al. Breath-hold CT attenuation correction for quantitative cardiac SPECT. *EJNMMI Res* 2012;2:33.
- (14) Kovalski G, Israel O, Keidar Z, Frenkel A, Sachs J, Azhari H. Correction of heart motion due to respiration in clinical myocardial perfusion SPECT scans using respiratory gating. *J Nucl Med* 2007;48:630-6.
- (15) Fricke H, Fricke E, Weise R, Kammeier A, Lindner O, Burchert W. A method to remove artifacts in attenuation-corrected myocardial perfusion SPECT Introduced by misalignment between emission scan and CT-derived attenuation maps. *J Nucl Med* 2004;45:1619-25.
- (16) Pan T, Lee TY, Rietzel E, Chen GT. 4D-CT imaging of a volume influenced by respiratory motion on multi-slice CT. *Medical physics* 2004;31:333-40.

- (17) Pan T, Mawlawi O, Luo D, Liu HH, Chi PC, Mar MV et al. Attenuation correction of PET cardiac data with low-dose average CT in PET/CT. *Medical physics* 2006;33:3931-8.
- (18) Kwiecinski J, Adamson PD, Lassen ML, Doris MK, Moss AJ, Cadet S et al. Feasibility of Coronary (18)F-Sodium Fluoride Positron-Emission Tomography Assessment With the Utilization of Previously Acquired Computed Tomography Angiography. *Circ Cardiovasc Imaging* 2018;11:e008325.
- (19) Dweck MR, Chow MW, Joshi NV, Williams MC, Jones C, Fletcher AM et al. Coronary arterial 18F-sodium fluoride uptake: a novel marker of plaque biology. *J Am Coll Cardiol* 2012;59:1539-48.
- (20) ClinicalTrials.gov. Effect of Evolocumab on Coronary Artery Plaque Volume and Composition by CCTA and Microcalcification by F18-NaF 2018.
- (21) Rubeaux M, Joshi NV, Dweck MR, Fletcher A, Motwani M, Thomson LE et al. Motion Correction of 18F-NaF PET for Imaging Coronary Atherosclerotic Plaques. *J Nucl Med* 2016;57:54-9.
- (22) Dey D, Schepis T, Marwan M, Slomka PJ, Berman DS, Achenbach S. Automated Three-dimensional Quantification of Non-calcified Coronary Plaque from Coronary CT Angiography: comparison with Intravascular Ultrasound Radiology 2010;257:516-22.
- (23) Moss AJ, Doris MK, Andrews JPM, Bing R, Daghem M, van Beek EJR et al. Molecular Coronary Plaque Imaging Using (18)F-Fluoride. *Circ Cardiovasc Imaging* 2019;12:e008574.
- (24) Lassen ML, Kwiecinski J, Cadet S, Dey D, Wang C, Dweck MR et al. Data-Driven Gross Patient Motion Detection and Compensation: Implications for Coronary (18)F-NaF PET Imaging. *J Nucl Med* 2019;60:830-6.
- (25) Chin BB, Nakamoto Y, Kraitchman DL, Marshall L, Wahl R. PET-CT evaluation of 2-deoxy-2-[18F]fluoro-D-glucose myocardial uptake: effect of respiratory motion. *Molecular imaging and biology : MIB : the official publication of the Academy of Molecular Imaging* 2003;5:57-64.
- (26) Goerres GW, Burger C, Kamel E, Seifert B, Kaim AH, Buck A et al. Respiration-induced attenuation artifact at PET/CT: technical considerations. *Radiology* 2003;226:906-10.
- (27) Goerres GW, Kamel E, Heidelberg TN, Schwitter MR, Burger C, von Schulthess GK. PET-CT image co-registration in the thorax: influence of respiration. *European journal of nuclear medicine and molecular imaging* 2002;29:351-60.
- (28) Beyer T, Antoch G, Blodgett T, Freudenberg LF, Akhurst T, Mueller S. Dual-modality PET/CT imaging: the effect of respiratory motion on combined image quality in clinical oncology. *European journal of nuclear medicine and molecular imaging* 2003;30:588-96.
- (29) Nakamoto Y, Osman M, Cohade C, Marshall LT, Links JM, Kohlmyer S et al. PET/CT: comparison of quantitative tracer uptake between germanium and CT transmission attenuation-corrected images. *J Nucl Med* 2002;43:1137-43.
- (30) Chi PC, Mawlawi O, Luo D, Liao Z, Macapinlac HA, Pan T. Effects of respiration-averaged computed tomography on positron emission tomography/computed tomography quantification and its potential impact on gross tumor volume delineation. *Int J Radiat Oncol Biol Phys* 2008;71:890-9.
- (31) Suzuki Y, Slomka PJ, Wolak A, Ohba M, Suzuki S, De Yang L et al. Motion-frozen myocardial perfusion SPECT improves detection of coronary artery disease in obese patients. *J Nucl Med* 2008;49:1075-9.
- (32) Dawood M, Buther F, Stegger L, Jiang X, Schober O, Schafers M et al. Optimal number of respiratory gates in positron emission tomography: a cardiac patient study. *Medical physics* 2009;36:1775-84.
- (33) Shechter G, Resar JR, McVeigh ER. Displacement and velocity of the coronary arteries: cardiac and respiratory motion. *IEEE Trans Med Imaging* 2006;25:369-75.

TABLES

Table 1

Age (SD)	66±10
Sex (Males)	21 (78%)
BMI (SD)	27±4
Hyperlipidemia	24 (89%)
Hypertension	14 (52%)
Diabetes	5 (18%)
Smoker/ex-smoker	7 (26%)
Total Plaque Volume (mm ³)	837 [620-1066]
Total NCP Volume (mm ³)	711 [55—859]
Total Calcified Volume (mm ³)	103 [43-205]

Continuous variables reported as mean ± SD or median [interquartile range]; categorical variables reported as n (%), BMI: Body mass index, NCP: Non-calcified plaque

FIGURES

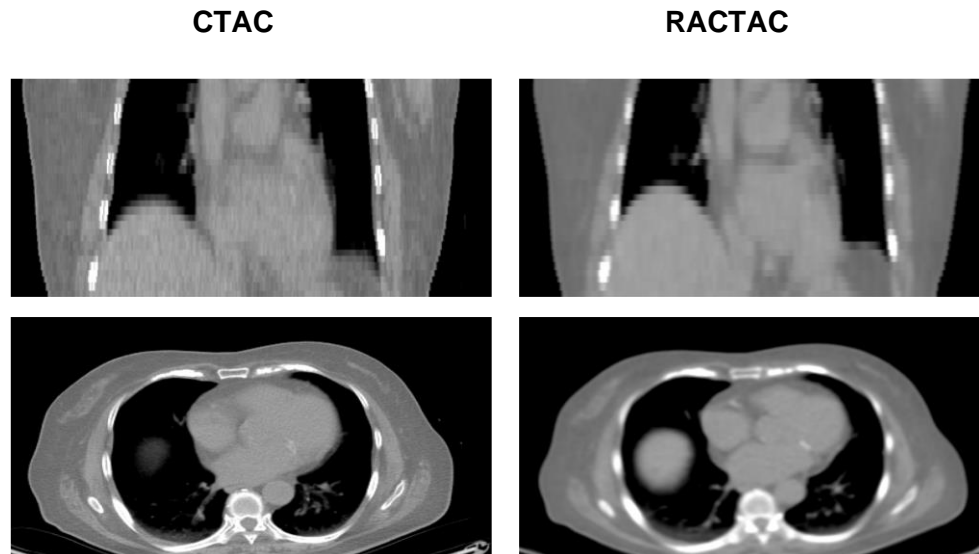


Figure 1 Standard attenuation map-CTAC (right) vs respiratory average CT attenuation maps-RACTAC (left). Coronal (top) and transverse (bottom) images.

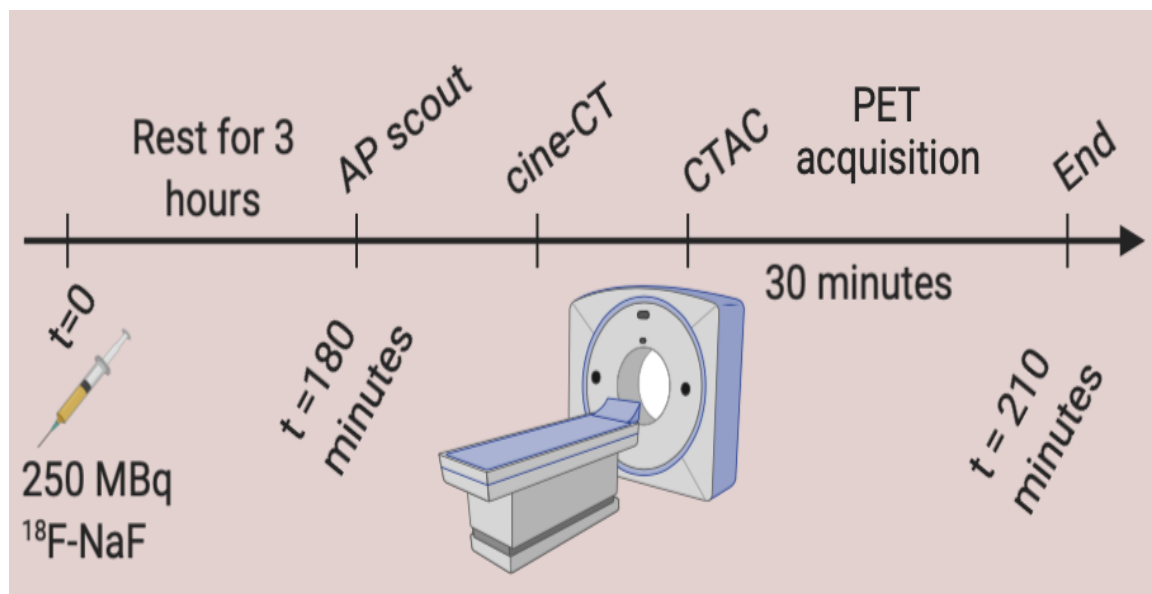


Figure 2 Imaging protocol for PET acquisition. All patients were scanned with arms positioned above the head.

AP: anteroposterior , CTAC: coronary tomography attenuation correction, PET: positron emission tomography

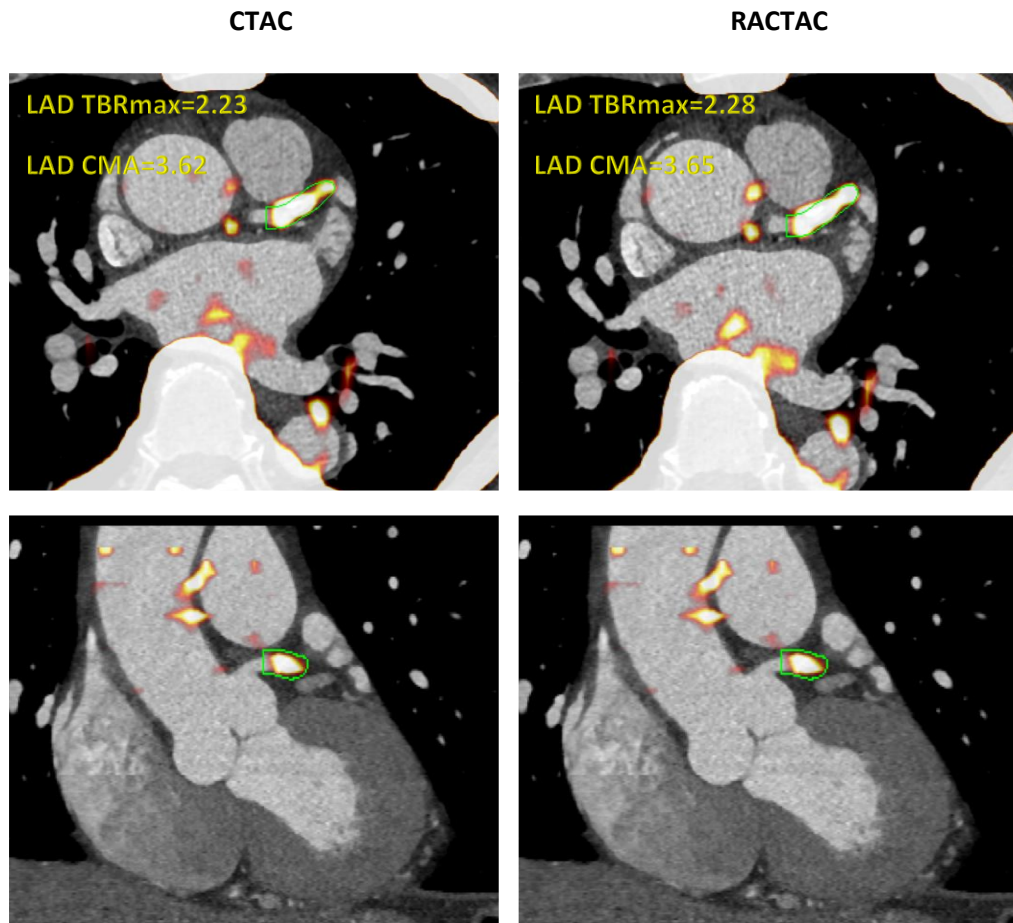


Figure 3 Left anterior descending artery ^{18}F -NaF uptake. Left panel shows fused CTA and PET images reconstructed using the CTAC maps, whereas shows the same CTA fused with PET an image reconstructed using RACTAC. There is good agreement between the measurements.

CTA = computed tomography angiography, CTAC = Computed Tomography Attenuation Correction and RACTAC = Respiratory averaged computed tomography attenuation correction.

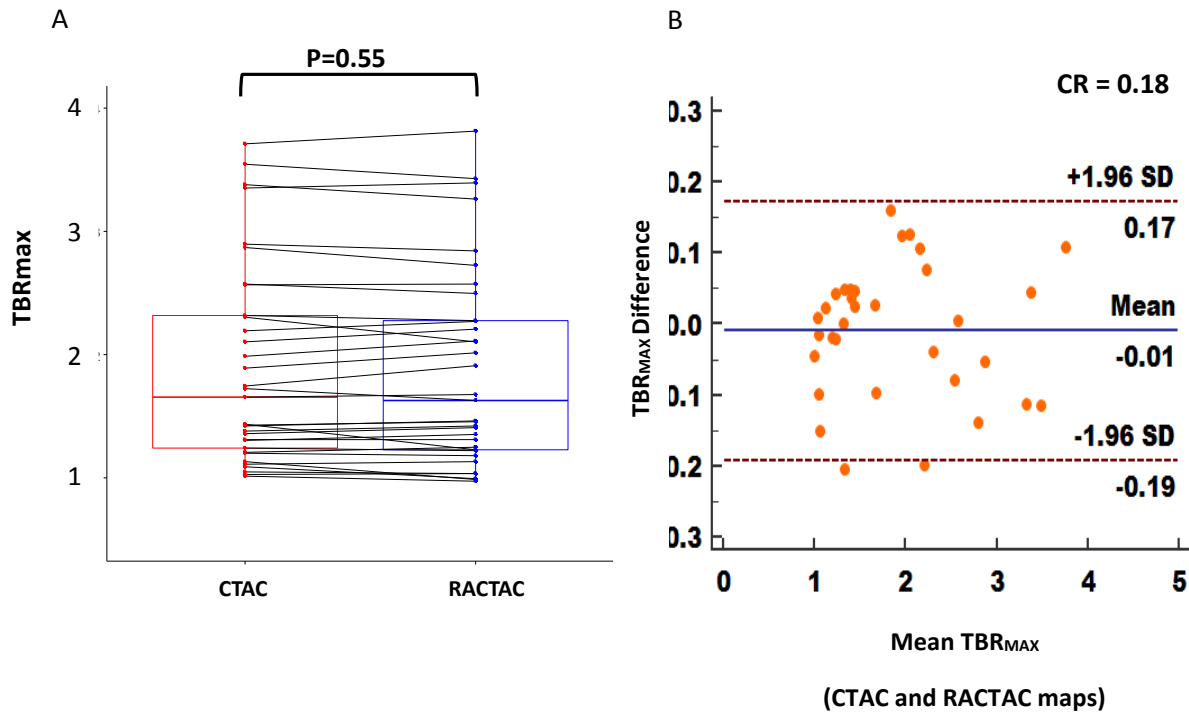


Figure 4 A) Boxplot with connecting lines between the TBR_{max} measurements using the RACTAC maps vs CTAC maps (blue and red boxes represent interquartile range, with a thick solid line inside represents the median), B) Bland-Altman plot of the differences between the TBR_{max} measured using RACTAC maps vs CTAC maps.

TBR_{max} = maximum Target to background ratio, CTAC = Computed Tomography Attenuation Correction and RACTAC = Respiratory averaged computed tomography attenuation correction, CR = coefficient of reproducibility

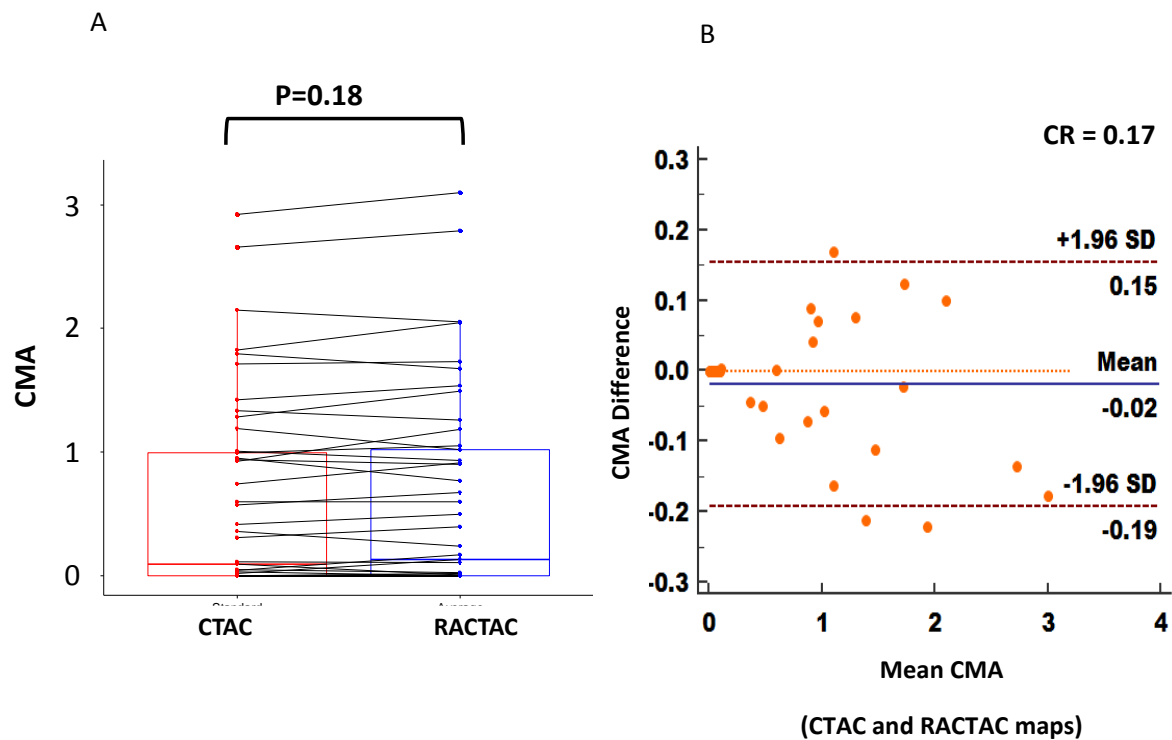


Figure 5 A) Boxplot with connecting lines between the CMA measurements using the RACTAC maps vs CTAC maps (blue and red boxes represent interquartile range, with thick solid line inside represents the median), B) Bland-Altman plot of the differences between the CMA measured using RACTAC maps vs CTAC maps.

CMA = coronary microcalcification activity, CTAC = Computed Tomography Attenuation Correction and RACTAC = Respiratory averaged computed tomography attenuation correction, CR = coefficient of reproducibility

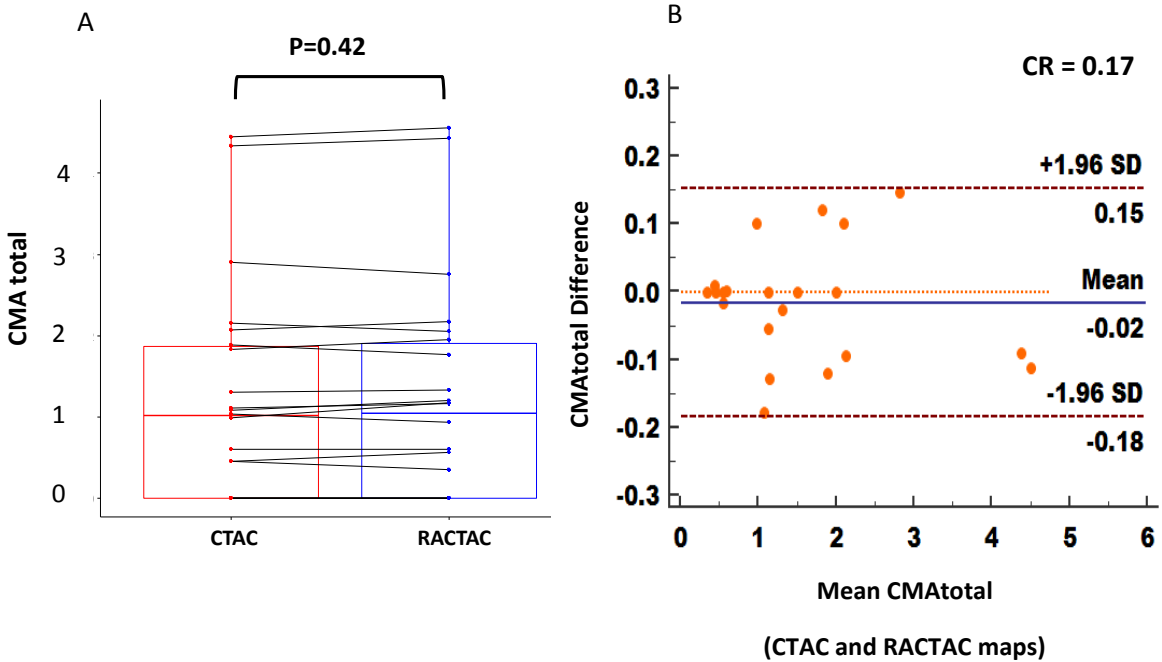


Figure 6 A) Boxplot with connecting lines between the CMA total measurements using the RACTAC maps vs CTAC maps (blue and red boxes represent interquartile range, with thick solid line inside represents the median), B) Bland-Altman plot of the differences between the CMAtotal measured using RACTAC maps vs CTAC maps.

CMAtotal = whole coronary tree microcalcification activity, CTAC = Computed Tomography Attenuation Correction and RACTAC = Respiratory averaged computed tomography attenuation correction, CR = coefficient of reproducibility